MAJOR ARTICLE

Alanylation of Teichoic Acids Protects *Staphylococcus aureus* against Toll-like Receptor 2–Dependent Host Defense in a Mouse Tissue Cage Infection Model

Sascha A. Kristian,[1,2,4] Xavier Lauth,[3] Victor Nizet,[3] Friedrich Goetz,[1] Birgid Neumeister,[2] Andreas Peschel,[1] and Regine Landmann[4]

[1]Microbial Genetics, University of Tübingen, and [2]Department of Transfusion Medicine, University Hospitals Tübingen, Tübingen, Germany; [3]Division of Pediatric Infectious Diseases, University of California, San Diego; [4]Division of Infectious Diseases, Department of Research, University Hospitals Basel, Basel, Switzerland

Staphylococcus aureus is inherently resistant to cationic antimicrobial peptides because of alanylation of cell envelope teichoic acids. To test the effect of alanylated teichoic acids on virulence and host defense mediated by Toll-like receptor 2 (TLR2), wild-type *(wt) S. aureus* ATCC35556 (*S.a.*113) and its isogenic mutant expressing unalanylated teichoic acids *(dlt⁻)* were compared in a tissue cage infection model that used C57BL/6 *wt* and TLR2-deficient mice. The minimum infective doses (MID) to establish persistent infection with *S.a.*113 were 10^3 and 10^2 colony-forming units (cfu) in wt and TLR2$^{-/-}$ mice, respectively. The corresponding MID for *dlt⁻* were 5×10^5 and 10^3 cfu in *wt* and TLR2$^{-/-}$ mice, respectively. Both mouse strains showed bacterial-load–dependent inflammation with elevations in tumor necrosis factor, macrophage inflammatory protein 2, and leukocytes, with increasing proportions of dead cells. These findings indicate that alanylated teichoic acids contribute to virulence of *S. aureus,* and TLR2 mediates host defense, which partly targets alanylated teichoic acids.

Staphylococcus aureus is a leading cause of community-acquired infections of the skin, soft tissue, musculoskeletal system, respiratory tract, and endovascular system, as well as hospital-acquired bacteremias and device-associated infections [1]. As a prerequisite to establishing invasive infection, *S. aureus* has evolved means to circumvent host defenses [1–3]. These host defense recognition and evasion strategies of *S. aureus* are incompletely understood [4].

Cationic antimicrobial peptides (CAMPs), such as defensins, cathelicidins, and thrombocidins, represent an important oxygen-independent defense mechanism of the innate immune system of mammals to combat invading pathogens [5, 6]. Defensins are found in various human tissues and in neutrophils [7]; cathelicidins, including human LL-37 and mouse cathelin-related antimicrobial peptide (CRAMP) [8], are produced by keratinocytes and polymorphonuclear neutrophils (PMNs). *S. aureus* is inherently resistant to the antimicrobial action of defensins [3, 9] and other CAMP [3]. Esterification of cell-envelope components with amino acids most likely represents one important determinant of this resistance [5]; such modifications lead to a decrease in the net negative surface charge of the bacteria and consequently to the repulsion of CAMP [10, 11].

We have previously described an operon on the *S. aureus* chromosome, *dltABCD,* the products of which

catalyze the introduction of D-alanine into teichoic acids, staphylococcal cell envelope polymers [10]. We showed that *S. aureus dlt* knockout *(dlt⁻)* bacteria are highly susceptible to isolated CAMP and oxygen-independent killing mechanisms of neutrophils in vitro [12]. Both *S. aureus* and *Listeria monocytogenes dlt⁻* bacteria were shown to be virulence attenuated in murine sepsis models [12, 13]. However, it remained unproven whether this virulence attenuation reflected the ability of teichoic acid alanylation to protect the bacteria from leukocyte-dependent killing in vivo. To specifically address this key issue, the present study compared the virulence of *S. aureus* wild-type and *dlt⁻* bacteria in a mouse tissue cage infection model [14, 15]. This model was chosen because it reproduces the common characteristics of device-associated infections where *S. aureus* is among the most frequently isolated pathogens [16]. These infections are characterized by a low initial infecting inoculum of microorganisms, by the absence of spread beyond the vicinity of the foreign body, and by a chronic evolution until removal of the prosthesis [15]. A potential reason for the persistence of infection is biofilm formation by the bacteria. Because *dlt⁻* bacteria exhibit a dramatic reduction in their ability to colonize artificial surfaces and to form biofilm in vitro [17], additional interest to study the virulence of *dlt⁻ S. aureus* in the tissue cage system is provided. We adapted the guinea pig tissue cage model [14, 18, 19] for the mouse, in which leukocyte host-defense mechanisms can be monitored and animals with targeted gene deletions are available for functional studies.

Finally, to identify precise molecular mechanisms by which teichoic acid alanylation allows *S. aureus* to evade host defense, we selected the host pattern recognition receptor Toll-like receptor 2 (TLR2) for study [20, 21]. When studied in vitro, TLR2 confers responsiveness of host leukocytes to heat-killed, gram-positive bacteria, including *S. aureus,* and to purified cell walls, peptidoglycan, lipoteichoic acid (LTA), or bacterial lipoproteins. After stimulation with these components, TLR2 mediates NF-κB translocation [22, 23] and cytokine or defensin release [24, 25]. A protective role of TLR2 has been demonstrated in murine models of *S. aureus* sepsis [26] and *Streptococcus pneumoniae* meningitis [27]. However, it is not known which TLR2 ligand plays the major role in *S. aureus*–induced inflammation in vivo and whether TLR2 participates in nonoxidative antimicrobial defense mechanisms to which *S. aureus* with unalanylated teichoic acids are particularly sensitive. These questions were addressed by comparing the host inflammatory response to wild-type *(wt)* and *dlt⁻ S. aureus* in C57BL/6 *wt* and TLR2⁻/⁻ mice.

MATERIALS AND METHODS

Preparation of staphylococcal strains. *S. aureus* ATCC35556 (*S.a.*113) [28] and isogenic *dltA⁻* bacteria were used for ex-

perimental infection of the animals. The procedures used for disruption of the *dltABCD* operon, for plasmid construction, and for phenotypic and genotypic characterizations of *dlt⁻* have been described in detail elsewhere [10]. The staphylococcal strains were grown overnight in tryptic soy broth at 37°C without shaking, subsequently washed 3 times in large volumes of 0.9% NaCl (pH 7.4), and resuspended in saline immediately before use.

Mice and tissue cage model. We kept 12–16-week-old female C57BL/6 *wt* mice (purchased from RCC) and TLR2⁻/⁻ mice, which had been backcrossed for 6 generations on a C57BL/6 background, under specific pathogen–free conditions in the Animal House of the Department of Research, University Hospitals Basel, according to the regulations of the Swiss veterinary law. Mice were anesthetized via intraperitoneal injection of 100 mg/kg ketamine (Ketalar; Warner-Lambert) and 20 mg/kg xylazinum (Xylapan; Graeub), and a sterile tissue cage was implanted subcutaneously in the back [29, 30]. The cages (internal and external diameters, 8 and 10 mm, respectively; length, 30 mm; internal volume, 1.84 mL) were identical to those used in the guinea pig foreign body infection model, as described elsewhere [15], and consisted of closed polytetrafluoroethylene Teflon cylinders with 130 regularly spaced 0.2-mm holes and contained 8-sinter glass beads. After surgery, mice were treated with buprenorphine (2 mg/kg subcutaneously twice daily) for 48 h to treat postoperative pain.

Two weeks after surgery, sterility of the tissue cage was verified, and 200 μL of suspensions of *S. aureus* was injected percutaneously with 25-gauge needles. As reported with tissue cage infections in guinea pigs [15], mice never developed bacteremia and showed no weight change during 3 weeks of infection.

Immunosuppression of mice with cyclophosphamide. Mice were treated with cyclophosphamide (200 mg/kg intraperitoneally [ip]) or as control with saline (ip) every 48 h starting 2 days before experimental infection.

Sampling of tissue cage fluid (TCF). Mice were anesthetized by inhalation of isofluorane (Abbott); 150-μL samples of TCF were drawn by percutaneous aspiration and transferred into sterile microreaction tubes containing 15 μL of 0.9% NaCl and 1.5% EDTA (pH 7.4), to avoid clotting. In selected experiments, the pH of TCF samples was measured with pH indicator strips (Merck).

Quantification of planktonic and adherent bacteria. To determine the load of planktonic (free-floating) bacteria in TCF, serial dilutions of the samples were plated on Mueller-Hinton broth (MHB) agar plates. Colony-forming units were enumerated after 24-h incubation at 37°C. To quantify the number of adherent staphylococci in the Teflon cages and on the glass beads, we used a method described elsewhere [31]. In brief, mice were killed, and tissue cages were explanted under sterile conditions 6 h to 21 days after infection. Glass beads and cages

were washed 3 times with saline and separately transferred into glass tubes containing 2–4 mL of 0.9% NaCl, EDTA (0.15%), and Triton-X (0.1%) (pH 7.4). The tubes were vortexed vigorously for 3×15 s, placed into an ultrasonic bath, and sonicated for 3 min at 200 W (Labsonic 2000; Bender & Hohbein). More than 95% of adherent *S. aureus* can be detached by this procedure [15]. After additional vortexing, appropriate volumes of serial dilutions were spread on MHB agar plates to quantify colony-forming units.

Counting of leukocytes, quantification of viable leukocytes, and identification of cell type in TCF. Leukocytes were quantified with a Coulter counter (Coulter Electronics). The percentage of viable leukocytes was assessed by trypan blue exclusion. Leukocyte differentiation in TCF was performed by Diff-Quick (Dade Behring) staining of cytospins and examination under high-power light microscopy.

Leukocyte viability in infected TCF. TCF of uninfected and infected mice (14 days after infection) was pooled separately and centrifuged at 400 *g* for 10 min to remove cellular host components. Infected TCF was rendered free of residual thrombocytes and bacteria by centrifugation for 5 min at 25,000 *g*. Pelleted cells of uninfected TCF were then resuspended in supernatants of infected cell-free TCF. After 6-h incubation at 37°C with gentle shaking in sterile 14-mL polypropylene tubes, the viability of leukocytes was assessed as described above.

Cytokine assays. Measurement of tumor necrosis factor (TNF) and macrophage inflammatory protein (MIP)–2 in the supernatants of the samples were carried out by sandwich ELISAs that used the OptEIA mouse TNF set (PharMingen) and the Quantikine M mouse MIP-2 set (R&D Systems), respectively.

FACScan analysis. Phenotypes of TCF leukocytes were analyzed by FACS after staining with the following antibodies [32]: anti-CD11b (MAC-1; Pharmingen) and anti-CD16/CD32 (FcγII/III receptor; Pharmingen). Rat IgG2b (Pharmingen) was used as isotype control. Fluorescein-conjugated goat anti–rat IgG (Jackson Laboratories) was used as secondary antibody.

In vitro growth of staphylococci in TCF. *S.a.*113 and *dlt⁻* bacteria were grown and washed as described above and adjusted to $\sim 5 \times 10^3$ cfu/mL in 100-μL pooled uninfected TCF, from which cellular components were removed by centrifugation at 400 *g* for 10 min and incubated at 37°C without shaking. After 24 h, 50 μL of serial dilutions was spread on MHB agar plates to quantify colony-forming units.

Susceptibility of **S.a.***113 and* **dlt⁻** *to gallidermin and CRAMP.* For bacterial susceptibility testing to gallidermin, TCF of *wt* or TLR2⁻/⁻ mice containing *S.a.*113 or *dlt⁻* was drawn 3 weeks after infection. In parallel, in vitro cultures of *S.a.*113 and *dlt⁻* were grown in tryptic soy broth and washed as described above. Bacteria were adjusted to $1–2 \times 10^4$ cfu/mL by dilution in saline. We plated 100 μL of this suspension on agar containing 0–8 μg/mL gallidermin and incubated them

for 24 h at 37°C. Determination of the MIC and MBCs of CRAMP against *S.a.*113 or *dlt⁻* bacteria was performed as described elsewhere for *Streptococcus pyogenes* [33].

Statistical analysis. Results of bacterial growth, TNF and MIP-2 levels, leukocyte numbers, and proportion of leukocytes alive were compared by analysis of variance for repeated measurements. $P < .05$ was considered to be statistically significant.

RESULTS

Staphylococcal growth in* wt *mice infected with* S.a.*113 or* dlt⁻ *bacteria. Our previous results in a mouse sepsis model revealed attenuated virulence of *S. aureus dltA* knockout bacteria *(dlt⁻)*, which lack D-alanine modifications in teichoic acids, compared with *wt S. aureus* [12]. To characterize local host defense mechanisms to which *dlt⁻* bacteria are more susceptible than *wt S. aureus* (*S.a.*113), we adapted a guinea pig tissue cage model [14, 15, 19] to the mouse. Tissue cages implanted in *wt* mice were experimentally infected with *S.a.*113 or *dlt⁻*, and the course of disease was compared over a period of 3 weeks. Tissue cage infections in guinea pigs can be established with a low inoculum (e.g., 100–1000 cfu) for most *S. aureus* strains [15]. Similarly, the minimum infective dose (MID) of *S.a.*113 for induction of persistent infections in *wt* mice was found to be low (1×10^3 cfu). In subsequent experiments, an inoculum of to $5.3 \pm 2.7 \times 10^3$ cfu of *S.a.*113 was used to ensure colonization of tissue cages. *S.a.*113 showed in vivo growth and persistence in 10 of 10 experiments (figure 1), multiplied to 1×10^6 cfu/mL within 3 days, and reached a plateau of growth at around 5×10^7 cfu/mL within 6–9 days. It remained at a constant density until day 21. In contrast to *S.a.*113, *dlt⁻* bacteria were cleared from tissue cages in all experiments ($n = 7$) after delivery of a similar inoculum ($7.7 \pm 2.3 \times 10^3$ cfu). In 6 of 7 experiments, no bacteria could be detected in TCF within 2 days (figure 1).
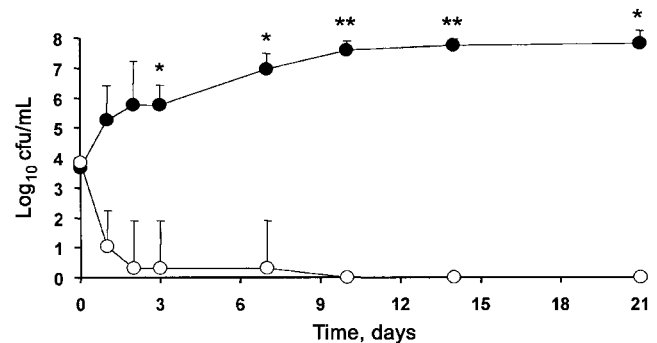

Figure 1. In vivo bacterial growth for 21 days after infection with $5.3 \pm 2.7 \times 10^3$ or $7.7 \pm 2.3 \times 10^3$ cfu of either *Staphylococcus aureus* ATCC35556 (*S.a.*113) (●) or *S. aureus* ATTC35556 *dltA* knockout bacteria (*dlt⁻*) (○), respectively. Data are mean ± SD from at least 7 experiments. *$P < .05$; **$P < .005$ (analysis of variance repeated measurements).
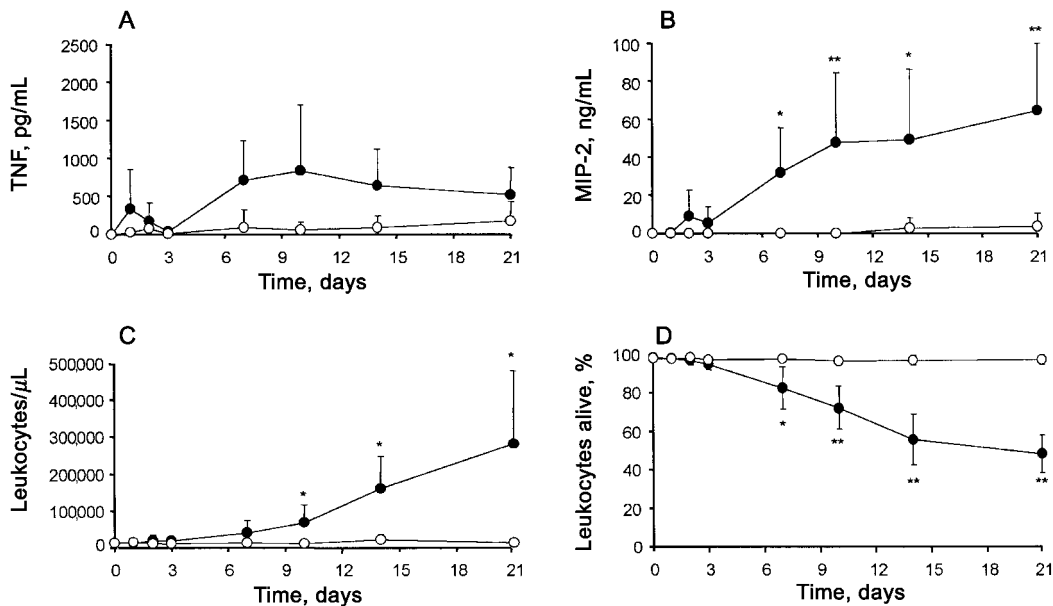
Figure 2. Tumor necrosis factor (TNF) concentration *(A)*; macrophage inflammatory protein (MIP)–2 concentration *(B)*; leukocyte count *(C)*; and proportion of viable leukocytes *(D)* in tissue cage fluid 21 days after infection with either *Staphylococcus aureus* ATCC35556 (*S.a.*113) (●) or *S. aureus* ATTC35556 *dltA* knockout bacteria (*dlt⁻*) (○) bacteria. Data are mean ± SD of at least 7 experiments in each group. *$P < .05$; **$P < .005$ (analysis of variance repeated measurements).

Quantification of planktonic bacteria does not take into account bacteria adhering to the inner surface of the implants and on the glass beads in the cages. Moreover, in the guinea pig model, staphylococci were shown to persist on the tissue cage surface, despite sterile TCF [34]; therefore, surface-adherent *S.a.*113 and *dlt⁻* bacteria were quantified 3–21 days after infection (data not shown). Surface-adherent bacteria were never found in the presence of sterile TCF, indicating that *wt* mice infected with *dlt⁻* bacteria were completely cured within 1–6 days. Samples from the bacterial preparations of the 2 staphylococcal strains grew equally well in MHB in vitro, indicating a similar fitness before infection (data not shown).

Because we did not obtain infection with 10^3 cfu of *dlt⁻*, the MID of *dlt⁻* was ascertained by serially increasing the inoculum in log steps. The *dlt⁻* inoculum necessary to establish a persistent infection was found to be between 5×10^5 and 1×10^6 cfu, 500–1000-fold higher than the MID of *S.a.*113. Infective doses of *dlt⁻* bacteria showed growth behavior similar to *S.a.*113 (data not shown), excluding differences in bacterial replication responsible for the disparity in MID. The higher MID of *dlt⁻* bacteria in the tissue cage model identifies teichoic acid alanylation as a virulence factor of *S. aureus* in foreign body infections.

Phenotypic and functional host responses of wt mice during infection with* S.a.*113 or* dlt⁻. To understand the contribution of host inflammatory responses to differences in vivo survival of *S.a.*113 and *dlt⁻*, several parameters of host response were monitored in *wt* mice inoculated with the above-men-

tioned $5{-}8 \times 10^3$ cfu of either bacterial strain. Leukocyte viability was evaluated, because killing of eukaryotic cells by staphylococci is known to occur [35]. Baseline leukocyte counts in the range of $1.4 \times 10^4 \pm 4.6 \times 10^3$ cells/μL were found in uninfected tissue cages and they were composed of a larger PMNs (70% ± 6%) and a smaller monocyte (24% ± 6%) fraction. These results are in agreement with those of previous reports [14, 30].

TNF release into *S.a.*113-infected cages was biphasic (figure 2*A*). A first peak with a mean value of 500 pg/mL was observed on day 1 in 5 of 10 mice, and a second peak with values between 800 and 1000 pg/mL occurred between days 7 and 10. After infection with *dlt⁻*, only 3 of 7 mice had detectable TNF elevations; the average levels of TNF were much lower than after *S.a.*113 infection (figure 2*A*). Thus, TNF release correlated with the level and persistence of the bacterial load.

Leukocyte activation was further assessed by measuring expression of the cell surface receptors CD11b, representing the β-chain of the complement receptor CR3, and CD16/CD32, which is representative of FcγII/III receptors. Both receptors, which are involved in phagocytosis [36] and expressed in mononuclear and PMNs cage leukocyte populations, were measured before and 24 h after infection. The percentage of CD11b- and CD16/CD32-positive leukocytes remained constant at 90% and 96%, respectively, after infection with either *S.a.*113 or *dlt⁻* bacteria. The mean fluorescence intensity of CD11b-positive cells increased 1.39 ± 0.28-fold and 1.42 ± 0.13-fold 24 h after infection in *S.a.*113- and *dlt⁻*-infected cages, respective-

ly, whereas the expression of CD16/CD32 remained unaltered (0.88 ± 0.14-fold and 1.05 ± 0.17-fold, respectively). The results indicate that complement receptor upregulation was triggered independently of the virulence potential of the bacteria.

In humans, neutrophil accumulation is induced by IL-8. IL-8 has not been found in mice, but MIP-2 may serve as a neutrophil chemotactic factor with homologous function, as shown in a murine lung injury model [37]. After infection with *S.a.*113, the concentrations of MIP-2 in TCF increased steadily from day 1 to day 21 (figures 2*B*). In contrast, the *dlt*⁻ mutant did not induce MIP-2, except for one mouse, which showed a modest release of MIP-2 beyond day 14 despite a sterile TCF. Elevated MIP-2 levels were followed by an influx of leukocytes into *S.a.*113-infected cages (figure 2*C*). The proportion of PMNs increased from $70\% \pm 6\%$ before infection to $83\% \pm 1\%$ between day 2 and day 21 after infection, corroborating a role for MIP-2 in neutrophil attraction in vivo. Cells migrated slowly into *S.a.*113-infected cages up to day 6 after infection but rapidly increased thereafter, culminating in a 26.7 ± 15.7-fold increase of total leukocyte numbers 21 days after infection. The leukocyte influx was completely absent (figure 2*C*), and the proportional changes among PMNs and monocytes did not appear (data not shown) in *dlt*⁻-infected tissue cages, which is in agreement with the low MIP-2 levels observed in these mice.

Beginning at day 3 after infection with *S.a.*113, when bacterial colony-forming unit and leukocyte counts had reached $\sim 1 \times 10^6$/mL and 2×10^4/μL, respectively, the proportion of viable leukocytes steadily decline from $95\% \pm 3\%$ to $48\% \pm 10\%$ through day 21 after infection (figure 2*D*). Because of the increasing proportions of dead cells, viable leukocyte numbers increased only 13-fold during the 3 weeks of infection. In contrast, all leukocytes in *dlt*⁻-infected cages remained alive. Cell death in cages infected with *S.a.*113 could not be attributed to an altered pH, because pH values remained constant at 7.8 ± 0.3 throughout the 21-day infection period. Furthermore, cell death was unlikely to be due to *S. aureus*–derived exotoxins [38], known to act rapidly [38], because uninfected cage leukocytes were not lysed during a 6-h incubation with infected cell-free TCF (data not shown).

In summary, several parameters of the host inflammatory response in the tissue cages were linked to growth and persistence of *S.a.*113 bacteria, absent in the *dlt*⁻-infected mice.

Role of leukocytes in host defense against* dlt⁻ *bacteria.
We showed that *S.a.*113 and *dlt*⁻ have similar growth properties in MHB medium in vitro. In contrast, we found the MID for *dlt*⁻ bacteria is much higher than that for *S.a.*113. We therefore tested whether *dlt*⁻ bacteria were more susceptible to soluble factors and/or to leukocytes present in TCF. *S.a.*113 and *dlt*⁻ grew similarly when cultured in vitro in TCF of uninfected mice after removing cellular components by centrifugation (data not shown). This finding indicates that the clearing of

dlt⁻ bacteria in wt mice was due to cell-associated host factors absent in uninfected, cell-free TCF.

To prove an essential role for leukocytes in clearance of *dlt*⁻ bacteria, *wt* mice were rendered leukopenic by means of the immunosuppressive drug cyclophosphamide. Cyclophosphamide injections reduced leukocyte numbers in uninfected cages by 75% to $3.5 \times 10^3 \pm 1.6 \times 10^3$ leukocytes/μL. As shown in figure 3, *dlt*⁻ bacteria were no longer cleared in leukopenic wt mice and grew at a similar rate as *S.a.*113. These results strongly suggest that leukocytes mediate the host defense against *S. aureus* in tissue cage infections.

Role of TLR2 in host defense against* dlt⁻ *bacteria.
TLR2⁻/⁻ mice were shown to be highly susceptible to infection by *S. aureus* [26] and *S. pneumoniae* [27]. We tested whether TLR2 participates in the immune defense against *S.a.*113 and *dlt*⁻ bacteria during tissue cage infection by comparing the course of disease in *wt* and TLR2⁻/⁻ mice. First, the MIDs for *S.a.*113 and *dlt*⁻ were determined in TLR2⁻/⁻ mice. The average MIDs of 10^2 cfu (*S.a.*113) and 10^3 cfu (*dlt*⁻) in TLR2⁻/⁻ mice (figure 4*A*) were 10-fold ($P < .05$) and 500–1000-fold lower, respectively, than those observed in *wt* mice (table 1). Thus, TLR2 is involved in murine host defense against *S. aureus* in tissue cage infections, and its role is prominent in the rapid clearance of *dlt*⁻ bacteria by *wt* mice. However, even in TLR2⁻/⁻ mice, *dlt*⁻ bacteria had a 10-fold higher MID than *S.a.*113 (table 1, figure 4*A*). This reflects a higher susceptibility of the mutant bacteria to additional host defense mechanisms not related to TLR2.

Course of disease in TLR2⁻/⁻ mice. To assess the evolution of infection in the absence of TLR2-mediated defense mechanisms, TLR2⁻/⁻ mice were infected with the same inocula of *S.a.*113 and *dlt*⁻ as used in the *wt* mice challenges. As shown in figure 4*B*, *S.a.*113 grew in TLR2⁻/⁻ mice and reached a plateau of growth 3 days after infection. The bacterial growth rate was faster than that observed in *wt* mice, where colony-
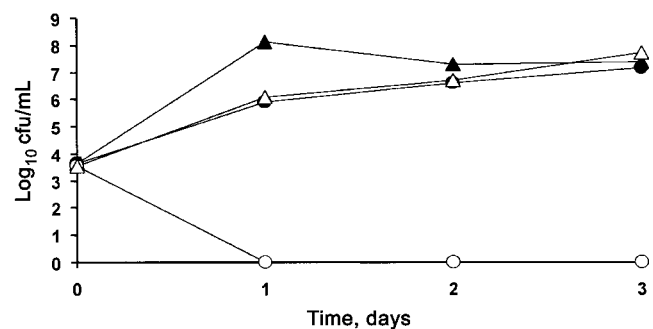

Figure 3. Effect of in vivo leukocyte depletion on bacterial growth in tissue cages. Growth of *Staphylococcus aureus* ATCC35556 (*S.a.*113) *(black symbols)* and *S. aureus* ATTC35556 *dltA* knockout bacteria (*dlt*⁻) *(white symbols)* bacteria in wild-type mice treated with saline *(circles)* or with cyclophosphamide *(triangles).* Results are colony-forming unit values of 1 representative experiment.
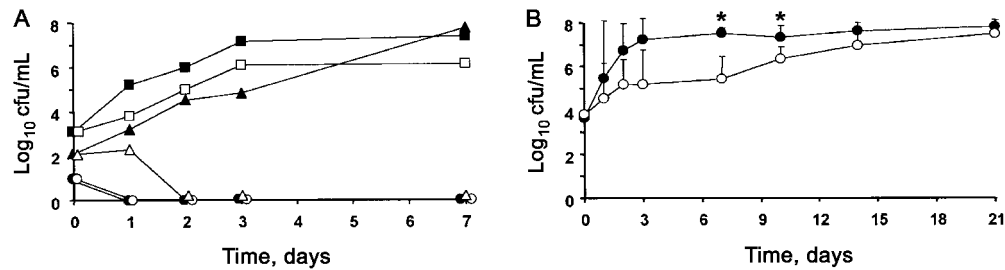
Figure 4. *A*, Determination of the minimum infective dose of *Staphylococcus aureus* ATCC35556 (*S.a.*113) and *S. aureus* ATTC35556 *dltA* knockout bacteria (*dlt⁻*) in Toll-like receptor 2 (TLR2)–deficient mice. Mice were infected with 10^1 cfu *(circles)*, 10^2 cfu *(triangles)*, or 10^3 cfu *(squares)* of *S.a.*113 *(black symbols)* or *dlt⁻* bacteria *(white symbols)*, respectively. Results of 1 representative experiment of 2 performed are shown. *B*, Effect of TLR2 deficiency on growth of *S.a.*113 (●) or *dlt⁻* bacteria (○). Data are the geometric mean of at least 7 experiments in each group. *$P < .05$ (analysis of variance repeated measurements).

forming unit counts were maximal only after 6–9 days (figures 4 and 1). The *dlt⁻* bacteria, which were cleared in *wt* mice (figure 1), proliferated in TLR2-deficient hosts ($n = 7$; figure 4*B*), thus identifying a role of TLR2 in murine immune defense against bacteria expressing unalanylated teichoic acids. Nevertheless, the *dlt⁻* bacteria showed significantly delayed growth, compared with *wt* bacteria ($P < .01$; figure 4*B*), reaching maximum levels on day 14—that is, 11 days later than *S.a.*113.

TCF from untreated TLR2$^{-/-}$ mice showed $1.1 \times 10^4 \pm 5.2 \times 10^3$ leukocytes/μL with 74% ± 9% PMNs and 17% ± 7% monocytes, which was similar to the values found in *wt* mice. Furthermore, bacterial replication in the tissue cage elicited an inflammatory response in the TLR2$^{-/-}$ host similar to that observed in *wt* mice. This response was characterized by increasing concentrations of TNF (figure 5*A*) and MIP-2 (figure 5*B*), by leukocyte influx (figure 5*C*), and by a decrease in leukocyte viability (figure 5*D*). However, for all parameters measured, infection with *S.a.*113 induced a stronger response than did infection with the *dlt⁻* mutant. The *S.a.*113-induced TNF response was biphasic, with a high peak after 1 day and a plateau from day 7 onward. In contrast, *dlt⁻* infection induced TNF only in the late phase, and average values were lower than in *S.a.*113-infected mice (figure 5*A*). MIP-2 was also induced faster and significantly more strongly in *S.a.*113-infected than in *dlt⁻*-infected TLR2$^{-/-}$ mice (figure 5*B*).

The delayed, weaker TNF and MIP-2 responses are most likely the consequence of the slower growth of the mutant bacteria in TLR2$^{-/-}$ mice. Infection in TLR2$^{-/-}$ mice was followed by leukocyte influx. Total leukocyte counts in *S.a.*113- and *dlt⁻*-infected cages increased 11.5 ± 6.4-fold and 12.8 ± 5.5-fold 21 days after infection, respectively (figure 5*C*). However, the maximum leukocyte concentration in TLR2$^{-/-}$ mice was lower (2.8×10^5 leukocytes/μL) than that in *wt* mice (5.9×10^5 leukocytes/μL; figure 2*C*). Leukocyte influx was also accompanied by a decreasing fraction of living cells (figure 4*E*). In *S.a.*113-infected cages, viability started to decline after day

2, whereas, in *dlt⁻*-infected cages, it started to decrease after day 7.

Susceptibility of S.a.*113 and* dlt⁻ *to antibacterial peptides.* CAMPs are deployed by the innate immune system in response to *S. aureus* infections. In a previous study, human PMNs exhibited a stronger bactericidal activity in vitro toward *dlt⁻* bacteria than on *wt S.a.*113 [12]. This difference paralleled the higher susceptibility of *dlt⁻* to CAMP [12]. It is known that TLRs participate in the induction of CAMP [25]. In tissue cages, the majority of the cells are PMNs, which are known to release a CAMP of the cathelicidin family, CRAMP [33]. Therefore, we compared the susceptibility of *S.a.*113 and *dlt⁻* bacteria to CRAMP in vitro. The MICs and MBCs of CRAMP were 4-fold lower for *dlt⁻*, compared with *S.a.*113 (figure 6*A*). To confirm a differential sensitivity of *S.a.*113 and *dlt⁻* bacteria to CAMP in vivo, the susceptibility of *S.a.*113 and *dlt⁻* to gallidermin, a CAMP of bacterial origin, was assessed after harvesting the bacteria from cages 3 weeks after infection. The gallidermin concentration required to kill 50% of the applied staphylococci was ~1 μg/mL for *S.a.*113 and <0.3 μg/mL for *dlt⁻* bacteria (figure 6*B*). This result supports a hypothesis that neutrophil-

Table 1. Minimum infective doses (MIDs) of *Staphylococcus aureus* in 2 kinds of mice.

	MID, cfu	
S. aureus strain	wt mice	TLR2$^{-/-}$ mice
*S.a.*113	1×10^3 ($n = 4$)	1×10^2 ($n = 3$)[a]
dlt⁻	5×10^5 to 1×10^6 ($n = 5$)	1×10^3 ($n = 2$)

NOTE. Average cfu counts, which caused a persistent infection, were set as MID. In each experiment, inocula ranging from 10^1 to 10^6 cfu were used to infect the tissue cages of wild-type and Toll-like receptor 2 deficient (TLR2$^{-/-}$) mice. *dlt⁻*, *S. aureus* ATTC35556*dltA* knockout bacteria; *S.a.*113, *S. aureus* ATCC35556; wt, C57BL/6 wild type.

[a] cfu counts required for infection were compared by Mann-Whitney *U* test; the difference for *S.a.*113 between wild-type and TLR2$^{-/-}$ mice was significant ($P < .05$).
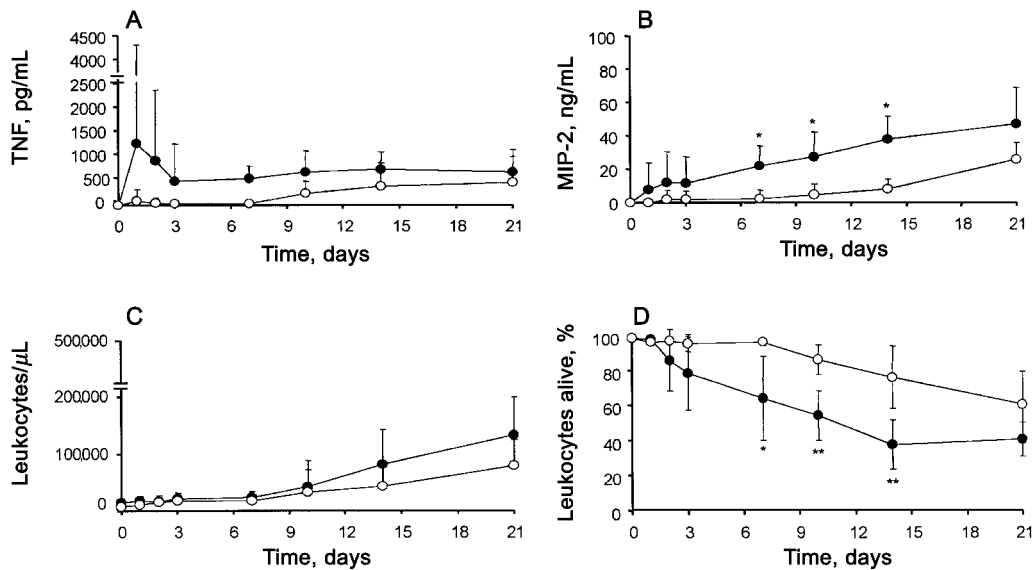
Figure 5. Course of disease in Toll-like receptor 2–deficient mice. *A,* Tumor necrosis factor (TNF) concentration; *B,* macrophage inflammatory protein (MIP)–2 concentration; *C,* leukocyte counts; *D,* leukocyte viability in tissue cages during 21 days after infection with *Staphylococcus aureus* ATCC35556 (*S.a.*113) (●) or *S. aureus* ATTC35556 *dltA* knockout bacteria (*dlt⁻*) (○) bacteria. Data are mean ± SD of at 7 least experiments in each group. *$P < .05$; **$P < .005$ (analysis of variance repeated measurements).

derived CAMP such as CRAMP could be responsible for the killing of *dlt⁻* bacteria in tissue cages in *wt* mice.

DISCUSSION

In the present study, we investigated the role of the *dltABCD*-mediated resistance against cationic antimicrobial host components in *S. aureus* virulence, and we investigated whether this immune escape mechanism protects against TLR2-dependent host defense. In a mouse tissue cage infection model, we found that alanylated teichoic acids protect against host defense—in large part, those pathways mediated by TLR2.

S. aureus teichoic acids mediate resistance against host defense by several mechanisms. Esterification of teichoic acids with amino acids decreases the net negative surface charge of the staphylococcal cells, thereby conferring resistance to CAMPs [10, 11] and other nonoxidative antimicrobial effector mechanisms, including phospholipase A₂ [39]. Indeed, *dlt⁻* bacteria with unalanylated teichoic acids are more susceptible to CAMP [10] and phospholipase A₂ [39]. Alanylation of teichoic acids also affects the capacity of the bacteria to adhere on glass and plastic surfaces; accordingly, *dlt⁻* bacteria exhibit reduced adhesion to artificial surfaces [17].

In this study, we investigated how alanylation of teichoic acids affect *S. aureus* survival during a local infection in vivo. Furthermore, teichoic acids were studied as potential targets of the pattern recognition receptor TLR2, prompted by the fact that purified LTA activates cells through TLR2 [22]. In contrast

to LTA, cell-wall teichoic acid has not yet been examined for its interaction with TLR2. *S. aureus* cell-wall teichoic acid differs from LTA in its lack of a lipid anchor and in the nature of its repeating sugar units. Yet, we hypothesize that TLR2 is engaged by both teichoic acid and LTA and that the TLR2-mediated effector mechanisms are influenced by the charge (i.e., alanylation) of the 2 components. TLR2 has 2 important functions: it transmits a proinflammatory signal in response to LTA, peptidoglycan, or lipoprotein stimulation [22, 23, 40]; and it exerts a protective role for the host during infection with *S. aureus* and other gram-positive bacteria. The mechanism of this protective role remains unknown.

We found that *dlt⁻* was less virulent than *wt S.a.*113, as determined by the 500–1000-fold higher MID of the mutant in *wt* mice. This finding indicates that the susceptibility to oxygen-independent antimicrobial host mechanisms facilitates bacterial clearing. Indeed, *dlt⁻* were more sensitive to CRAMP in vitro and gallidermin ex vivo. Future studies that use CRAMP⁻/⁻ mice, which lack the mouse neutrophil cathelicidin CRAMP [33], will address whether murine cathelicidins are responsible for clearing of *dlt⁻* in the tissue cage model. An increased sensitivity to phospholipase A₂, which we described recently for *dlt⁻* bacteria [39], could not explain clearing of the *dlt⁻* mutant in our model, because C57/BL6 mice are deficient in phospholipase A₂ [41]. It is also unlikely that *dlt⁻* bacteria were more sensitive to oxidative killing because they were cleared equally in vivo in the presence and absence of the free radical scavenger α-phenyl-ter-butylnitrone (data not shown),
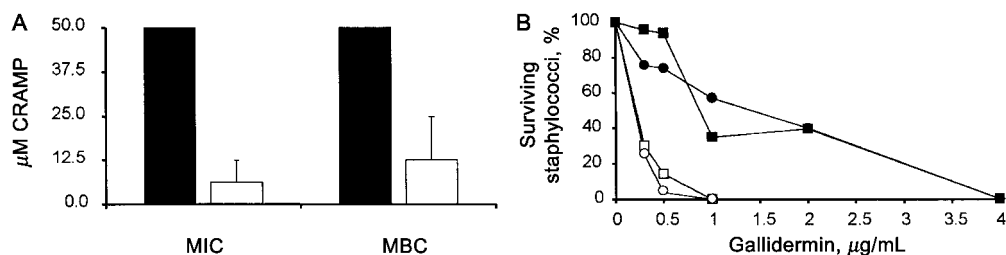
Figure 6. *A,* Susceptibility of *Staphylococcus aureus* ATCC35556 (*S.a.*113) *(black bars)* and *S. aureus* ATTC35556 *dltA* knockout bacteria *(dlt⁻)* *(white bars)* to mouse cathelicidin cathelin-related antimicrobial peptide (CRAMP), as assessed by the MIC and the minimum bactericidal concentration (MBC) in vitro. Studies were performed in duplicate. *B,* Susceptibility of *S.a.*113 *(black symbols)* and *dlt⁻* *(white symbols)* bacteria to gallidermin, grown in vivo *(circles)* or in vitro *(squares)*. Values of 1 representative experiment are expressed as percentages of cfu obtained on agar plates containing no gallidermin.

an agent known to effectively decrease oxidative injury in group B streptococcal meningitis [42]. Finally, clearing of *dlt⁻* bacteria is apparently not related to a reduced colonization on glass surfaces in vivo, because no differences were found between *S.a.*113 and *dlt⁻* in adhesion.

Because *dlt⁻* are more susceptible to CAMP, it was interesting to investigate whether innate receptors, which are known to contribute to CAMP release, participate in their elimination. TLR2 could play such a role, although so far only β-defensin was shown to be induced via TLR2 [25] and this induction was measured after stimulation with bacterial lipoprotein. Up-regulation of cathelicidin expression after infection with live bacteria occurs by an unknown mechanism. Future studies will address the question whether TLR2 modulates cathelicidin release. We found the MID of *dlt⁻* was 1000-fold lower in TLR2$^{-/-}$ mice than in *wt* mice. Although 10^5 to 10^6 cfu were required in *wt* mice, only 10^3 cfu caused an infection in TLR2$^{-/-}$ mice. This means that TLR2 recognition and/or effector mechanisms are important in the control of *dlt⁻* bacteria. Of interest, *dlt⁻* remained less virulent than *S.a.*113 in TLR2$^{-/-}$ mice, indicating that TLR2-independent mechanisms also contribute to bacterial clearance.

Whether TLR2 participates directly in bacterial clearance is not clear. It is unlikely that phagocytosis is influenced by TLR2, because zymosan uptake in macrophages was shown to be TLR2 independent [43]. It is possible that engagement of TLR2 leads to bacterial killing through an increased generation of CAMP, via reactive oxygen species or via release of chemokines that recruit additional leukocytes to the site of infection. Furthermore, TLR2 activation might induce killing via a nitric oxide–dependent mechanism, as shown during infection with *Mycobacterium tuberculosis* [44].

Our tissue cage model also demonstrates that TLR2 contributes moderately to efficient killing of *S.a.*113. The MID of *S.a.*113 was 10-fold lower in TLR2$^{-/-}$ mice than in *wt* mice. Early *S.a.*113 growth was faster in the absence of TLR2. Comparison of *S.a.*113 and *dlt⁻* in the 2 mouse strains implies that alanylated teicho-

ic acids protect *S. aureus* from TLR2-mediated defense. Three mechanisms not mutually exclusive can be envisaged. First, *dlt⁻* bacteria may bind to host cell TLR2 more strongly than *S.a.*113. Second, they may bind to other phagocytic receptors, which leads to efficient clearing only in the presence of TLR2. Third, both *S.a.*113 and *dlt⁻* may activate leukocytes to an equivalent degree, but the mutant may be killed faster and better because of its increased susceptibility to CAMP. It remains to be determined which of these mechanisms is TLR2 dependent.

Our results deserve 2 further comments. In tissue cage infection, the inflammatory response was very strong. However, the onset of the inflammatory response was delayed and strictly correlated with bacterial number. Release of MIP-2 and TNF showed a biphasic pattern. After 24 h of infection, small amounts of both mediators were detected, and these levels were not associated with cessation of bacterial growth. Of interest, this early initial peak was present in TLR2$^{-/-}$ mice and therefore is mediated by TLR2-independent mechanisms. We also found an increased expression of CR3 during the early stage of infection in both mouse strains, again independent of TLR2. The inflammation response in this model was then characterized by a second phase with release of extremely large amounts of MIP-2 and TNF, high leukocyte numbers, and massive leukocyte cell death. This delayed and apparently insufficient response appears when the bacteria reach high numbers and does not affect bacterial clearance. This phenomenon is likely a by-product of the closed infection model and might resemble the pathophysiology of implant-associated infection in humans.

A final comment concerns the association of *S. aureus* virulence with the expression of alanylated teichoic acids. In the tissue cage model, bacteria have a growth advantage as a consequence of the delayed inflammatory response. Nevertheless, *S. aureus* is immediately cleared when it expresses unalanylated teichoic acids that render them highly susceptible to the action of CAMP. Future strategies that target enzymes encoded by the *dltABCD* operon may be of benefit in therapy of *S. aureus* infection.

References

1. Lowy FD. *Staphylococcus aureus* infections. N Engl J Med **1998**; 339: 520–32.
2. Costerton JW, Stewart PS, Greenberg EP. Bacterial biofilms: a common cause of persistent infections. Science **1999**; 284:1318–22.
3. Peschel A, Collins LV. Staphylococcal resistance to antimicrobial peptides of mammalian and bacterial origin. Peptides **2001**; 22:1651–9.
4. Verhoef F. Host defense against infection. In: Crossley KB, Archer GL, eds. The staphylococci in human disease. New York: Churchill Livingstone, **1997**:213–2.
5. Peschel A. How do bacteria resist human antimicrobial peptides? Trends Microbiol **2002**; 10:179–86.
6. Yeaman MR, Bayer AS, Koo SP, Foss W, Sullam PM. Platelet microbicidal proteins and neutrophil defensin disrupt the *Staphylococcus aureus* cytoplasmic membrane by distinct mechanisms of action. J Clin Invest **1998**; 101:178–87.
7. Lehrer RI, Ganz T. Defensins of vertebrate animals. Curr Opin Immunol **2002**; 14:96–102.
8. Gallo RL, Kim KJ, Bernfield M, et al. Identification of CRAMP, a cathelin-related antimicrobial peptide expressed in the embryonic and adult mouse. J Biol Chem **1997**; 272:13088–93.
9. Harder J, Bartels J, Christophers E, Schroder JM. Isolation and characterization of human β-defensin–3, a novel human inducible peptide antibiotic. J Biol Chem **2001**; 276:5707–13.
10. Peschel A, Otto M, Jack RW, Kalbacher H, Jung G, Götz F. Inactivation of the *dlt* operon in *Staphylococcus aureus* confers sensitivity to defensins, protegrins, and other antimicrobial peptides. J Biol Chem **1999**; 274:8405–10.
11. Peschel A, Jack RW, Otto M, et al. *Staphylococcus aureus* resistance to human defensins and evasion of neutrophil killing via the novel virulence factor MprF is based on modification of membrane lipids with L-lysine. J Exp Med **2001**; 193:1067–76.
12. Collins V, Kristian SA, Weidenmaier C, et al. *Staphylococcus aureus* strains lacking D-alanine modifications of teichoic acids are highly susceptible to human neutrophil killing and are virulence-attenuated in mice. J Infect Dis **2002**; 186:214–9.
13. Abachin E, Poyart C, Pellegrini E, et al. Formation of D-alanyl-lipoteichoic acid is required for adhesion and virulence of *Listeria monocytogenes*. Mol Microbiol **2002**; 43:1–14.
14. Zimmerli W, Waldvogel FA, Vaudaux P, Nydegger UE. Pathogenesis of foreign body infection: description and characteristics of an animal model. J Infect Dis **1982**; 146:487–97.
15. Zimmerli W. Tissue cage infection model. In: Zak O, Sande MA, eds. Handbook of animal models of infection. San Diego: Academic Press, **1999**:409–17.
16. Vaudaux PPF, Lew DP, Waldvogel FA. Host factors predisposing to and influencing therapy of foreign body infections. In: Waldvogel FA, Bisno AL, eds. Infections associated with indwelling devices. Washington, DC: American Society for Microbiology Press, **2000**:1–26.
17. Gross M, Cramton SE, Götz F, Peschel A. Key role of teichoic acid net charge in *Staphylococcus aureus* colonization of artificial surfaces. Infect Immun **2001**; 69:3423–6.
18. Zimmerli W, Lew PD, Waldvogel FA. Pathogenesis of foreign body infection: evidence for a local granulocyte defect. J Clin Invest **1984**; 73:1191–200.
19. Vaudaux P, Grau GE, Huggler E, et al. Contribution of tumor necrosis factor to host defense against staphylococci in a guinea pig model of foreign body infections. J Infect Dis **1992**; 166:58–64.
20. Underhill DM, Ozinsky A. Toll-like receptors: key mediators of microbe detection. Curr Opin Immunol **2002**; 14:103–10.
21. Beutler B. Toll-like receptors: how they work and what they do. Curr Opin Hematol **2002**; 9:2–10.
22. Schwandner R, Dziarski R, Wesche H, Rothe M, Kirschning CJ. Peptidoglycan- and lipoteichoic acid–induced cell activation is mediated by toll-like receptor 2. J Biol Chem **1999**; 274:17406–9.
23. Opitz B, Schroder NW, Spreitzer I, et al. Toll-like receptor–2 mediates *Treponema* glycolipid and lipoteichoic acid–induced NF-κB translocation. J Biol Chem **2001**; 276:22041–7.
24. Aliprantis AO, Yang RB, Mark MR, et al. Cell activation and apoptosis by bacterial lipoproteins through toll-like receptor–2. Science **1999**; 285:736–9.
25. Birchler T, Seibl R, Buchner K, et al. Human Toll-like receptor 2 mediates induction of the antimicrobial peptide human β-defensin 2 in response to bacterial lipoprotein. Eur J Immunol **2001**; 31:3131–7.
26. Takeuchi O, Hoshino K, Akira S. Cutting edge: TLR2-deficient and MyD88-deficient mice are highly susceptible to *Staphylococcus aureus* infection. J Immunol **2000**; 165:5392–6.
27. Echchannaoui H, Frei K, Schnell C, Leib S, Zimmerli W, Landmann R. Toll-like receptor 2–deficient mice are highly susceptible to *Streptococcus pneumoniae* meningitis due to reduced bacterial clearing and enhanced inflammation. J Infect Dis **2002**; 186:798–806.
28. Iordanescu S, Surdeanu M. Two restriction and modification systems in *Staphylococcus aureus* NCTC8325. J Gen Microbiol **1976**; 96:277–81.
29. Dayer E, Yoshida H, Izui S, Lambert PH. Quantitation of retroviral gp70 antigen, autoantibodies, and immune complexes in extravascular space in arthritic MRL-lpr/lpr mice: use of a subcutaneously implanted tissue cage model. Arthritis Rheum **1987**; 30:1274–82.
30. Dawson J, Rordorf-Adam C, Geiger T, et al. Interleukin-1 (IL-1) production in a mouse tissue chamber model of inflammation. I. Development and initial characterisation of the model. Agents Actions **1993**; 38:247–54.
31. Zimmerli W, Frei R, Widmer AF, Rajacic Z. Microbiological tests to predict treatment outcome in experimental device-related infections due to *Staphylococcus aureus*. J Antimicrob Chemother **1994**; 33:959–67.
32. Cauwels A, Frei K, Sansano S, et al. The origin and function of soluble CD14 in experimental bacterial meningitis. J Immunol **1999**; 162: 4762–72.
33. Nizet V, Ohtake T, Lauth X, et al. Innate antimicrobial peptide protects the skin from invasive bacterial infection. Nature **2001**; 414:454–7.
34. Zimmerli W, Zak O, Vosbeck K. Experimental hematogenous infection of subcutaneously implanted foreign bodies. Scand J Infect Dis **1985**; 17: 303–10.
35. Gresham HD, Lowrance JH, Caver TE, Wilson BS, Cheung AL, Lindberg FP. Survival of *Staphylococcus aureus* inside neutrophils contributes to infection. J Immunol **2000**; 164:3713–22.
36. Underhill DM, Ozinsky A. Phagocytosis of microbes: complexity in action. Annu Rev Immunol **2002**; 20:825–52.
37. Tsujimoto H, Ono S, Mochizuki H, et al. Role of macrophage inflammatory protein 2 in acute lung injury in murine peritonitis. J Surg Res **2002**; 103:61–7.
38. Walev I, Weller U, Strauch S, Foster T, Bhakdi S. Selective killing of human monocytes and cytokine release provoked by sphingomyelinase (β-toxin) of *Staphylococcus aureus*. Infect Immun **1996**; 64:2974–9.
39. Koprivnjak T, Peschel A, Gelb MH, Liang NS, Weiss JP. Role of charge properties of bacterial envelope in bactericidal action of human group

IIA phospholipase A$_2$ against *Staphylococcus aureus*. J Biol Chem **2002**; 277:47636–44.

40. Lien E, Sellati TJ, Yoshimura A, et al. Toll-like receptor 2 functions as a pattern recognition receptor for diverse bacterial products. J Biol Chem **1999**; 274:33419–25.

41. Kennedy BP, Payette P, Mudgett J, et al. A natural disruption of the secretory group II phospholipase A$_2$ gene in inbred mouse strains. J Biol Chem **1995**; 270:22378–85.

42. Christen S, Schaper M, Lykkesfeldt J, et al. Oxidative stress in brain during experimental bacterial meningitis: differential effects of α-phenyl-tert-butyl nitrone and *N*-acetylcysteine treatment. Free Radic Biol Med **2001**; 31:754–62.

43. Underhill DM, Ozinsky A, Smith KD, Aderem A. Toll-like receptor–2 mediates mycobacteria-induced proinflammatory signaling in macrophages. Proc Natl Acad Sci USA **1999**; 96:14459–63.

44. Thoma-Uszynski S, Stenger S, Takeuchi O, et al. Induction of direct antimicrobial activity through mammalian toll-like receptors. Science **2001**; 291:1544–7.